

Synthesis and Characterization of Semi-Aliphatic Polyimide Films with Excellent Comprehensive Performance

Yang Wu^a, Chengcheng Ding^a, Juan Yu^{a,*}, and Pei Huang^a

^aNanjing Tech University, Nanjing, 211816 China

*e-mail: juanyu@njtech.edu.cn

Received December 8, 2022; revised January 23, 2023; accepted January 27, 2023

Abstract—Transparent polyimide films with excellent comprehensive properties may be indispensable to next-generation optoelectronic and flexible display applications. To date, the most studied transparent polyimide films are mainly prepared with alicyclic dianhydride as monomer, but the related properties of such films are not satisfactory. In this work, two series of highly optically transparent copolyimide films were prepared by the polycondensation of dicyclohexyl-3,4,3',4'-tetracarboxylic dianhydride, 1,2,4,5-cyclohexanetetracarboxylic dianhydride, 4,4'-(hexafluoroisopropylidene) diphthalic anhydride with 4,4'-oxydianiline via a facile one-step method. Through the optimization of structure and composition, the relationship between structure and properties of copolymerized semi-alicyclic polyimide was studied. The prepared copolyimide films show good thermal stability: glass transition temperatures in the range of 264–315°C and 5% weight loss temperature of 463–527°C, superior optical transparency up to 90%. Specifically, these copolyimide films have tensile strength greater than 90.3 MPa.

DOI: 10.1134/S1560090423700781

INTRODUCTION

Since its creation, polyimides (PI) have been utilized extensively for various applications due to superior thermal stability, mechanical characteristics, and chemical stability, which makes them distinguished from other polymer films [1–4]. The demand for PI films has increased along with science and technology advancements. Traditional PI films haven't been able to keep up with the demands of modern manufacturing, so a variety of functional PI materials have been continuously created and investigated [5–8].

In recent years, with the rapid development of flexible electronic industry represented by flexible sensors, photovoltaic devices and thin-film solar cells, the demand for polymeric optical films with superior optical transparency, thermal stability, and excellent mechanical properties is increasingly urgent [9–11]. However, the conventional fully aromatic PI films cannot be widely employed in the optical area due to their dark color and limited light transmission in the visible light region [12–15]. Alicyclic polyimides, polyolefin and polyester films have good light transmittance while their thermal stability and mechanical properties are not satisfactory, which also prevents them from being widely used. In fact, the poor optical properties of traditional aromatic PI films are influenced by the formation of intramolecular and intermolecular charge transfer [16–20]. That is to say, from

the standpoint of building molecular architectures, it is a feasible way to developing colorless polymer films with good thermal resistant, mechanical properties, and transparency [15].

The transparency of polyimide films can be increased in a variety of ways, such as introducing the high negative ion groups, large substituents, asymmetric structure, and alicyclic structure into the PI chains, which can decrease the absorption of visible light by preventing the development of intermolecular and intramolecular charge transfer [21–24]. Among all kinds of colorless polyimide (CPI) films reported in the literature so far, fluorine-containing aromatic and semi-alicyclic are the most important ones [14, 15, 17]. Because of the different ways to realize colorless and transparent, the properties of different kinds of CPI films are also significantly different. Alicyclic CPI films often show higher optical transmittance and lower curing temperature than fluorinated CPI films, however, poorer mechanical performance and thermal stability [25, 26]. For instance, Li et al. prepared CPI films using 1,2,4,5-cyclohexanetetracarboxylic dianhydride (HPMDA) and 4,4'-oxydianiline (ODA); however, its thermal stability was not satisfactory [14]. The thermal decomposition temperature was lower than 460°C for 5% weight loss. Wu et al. prepared CPI films using dicyclohexyl-3,4,3',4'-tetracarboxylic dianhydride (HBPDA) and ODA, which show high transparency, reaching 83.6% at 450 nm, however, its glass transition temperature T_g was only about 260°C

[27]. Alain and Cosutchi prepared CPI films with excellent heat resistance using 4,4'-(hexafluoroisopropylidene) diphthalic anhydride (6FDA) and ODA [28, 29]. However, the tensile strength was lower than 91 MPa, and the cut-off wavelength of the films is above 360 nm, indicating that their optical and mechanical properties are not excellent. Zhi and Lan reported CPI films with outstanding overall performance synthesized from a fluorine and alicyclic containing monomers, but their preparation cost was relatively high [15, 30]. Therefore, the research of CPI films with high optical transparency, good thermal stability, superior flexibility and low cost is an urgent problem to be solved in the field of flexible display.

In this work, we have prepared two representative CPI films with employing random copolycondensation of dianhydride and diamine monomers that are readily available on the market to overcome these problems mentioned above. The results of the experiments show that copolymer CPI films display excellent overall performance. It was possible to achieve a compromise between mechanical qualities, thermal stability, optical properties, dissolve performance and preparation cost.

EXPERIMENTAL

Materials

Dicyclohexyl-3,4,3',4'-tetracarboxylic dianhydride (98%), 1,2,4,5-cyclohexanetetracarboxylic dianhydride (97%), 4,4'-oxydianiline (98%), isoquinoline (97%), *N,N*-dimethylacetamide (DMAc, 99.8%, extra dry, with molecular sieves) were purchased from Energy Chemical Reagent Company. *m*-Cresol (99%), 4,4'-(hexafluoroisopropylidene) diphthalic anhydride (99%) were obtained from Shanghai Aladdin Reagent Company. Without any additional purification, all materials were utilized as received.

Co-PI Synthesis and Films Preparation

Typical synthesis process of polyimide is as follows. HPMDA (0.4528 g, 2.02 mmol), 6FDA (0.8974 g, 2.02 mmol), ODA (0.8010 g, 4 mmol), and isoquinoline (0.1 g) were dissolved in 12 g of *m*-cresol and continuously stirred for 30 min at 100°C under nitrogen atmosphere, then the mixtures were stirred at 180°C for 6 h. The experiment was also safer and easier by avoiding the use of toluene to remove the water generated in the system. After cooling to 120°C, solution was poured into a vigorously stirred ethanol solution to obtain the fibrous polymer. Polymer was extracted with ethanol solution for 24 h, changing every 8 h, and then dried under vacuum at 120°C for 12 h. Yield 2.04 g (95%). Other polymers are synthesized in a similar way as described above, except that the ratio of different dianhydrides differs. These co-PI films are designated R/6FDA-*n*m-ODA, R, *n* and *m* stand for hydrogenated dianhydride monomer, molar percent-

age of hydrogenated dianhydride monomer, molar percentage of 6FDA, respectively. See Scheme 1 for more details.

The dried fibrous polymer was redissolved in DMAc to make a mixed solution with a solid content of 20%. The mixture was cast onto a clean glass plate and then placed in a vacuum oven, which was subsequently dried at 90°C for 3 h, the procedure was continued under vacuum to increase the temperature according to the following process: stayed for 1.5 h at 130, 170, 210, and 250°C, respectively. The same process was used to prepare other co-PI films.

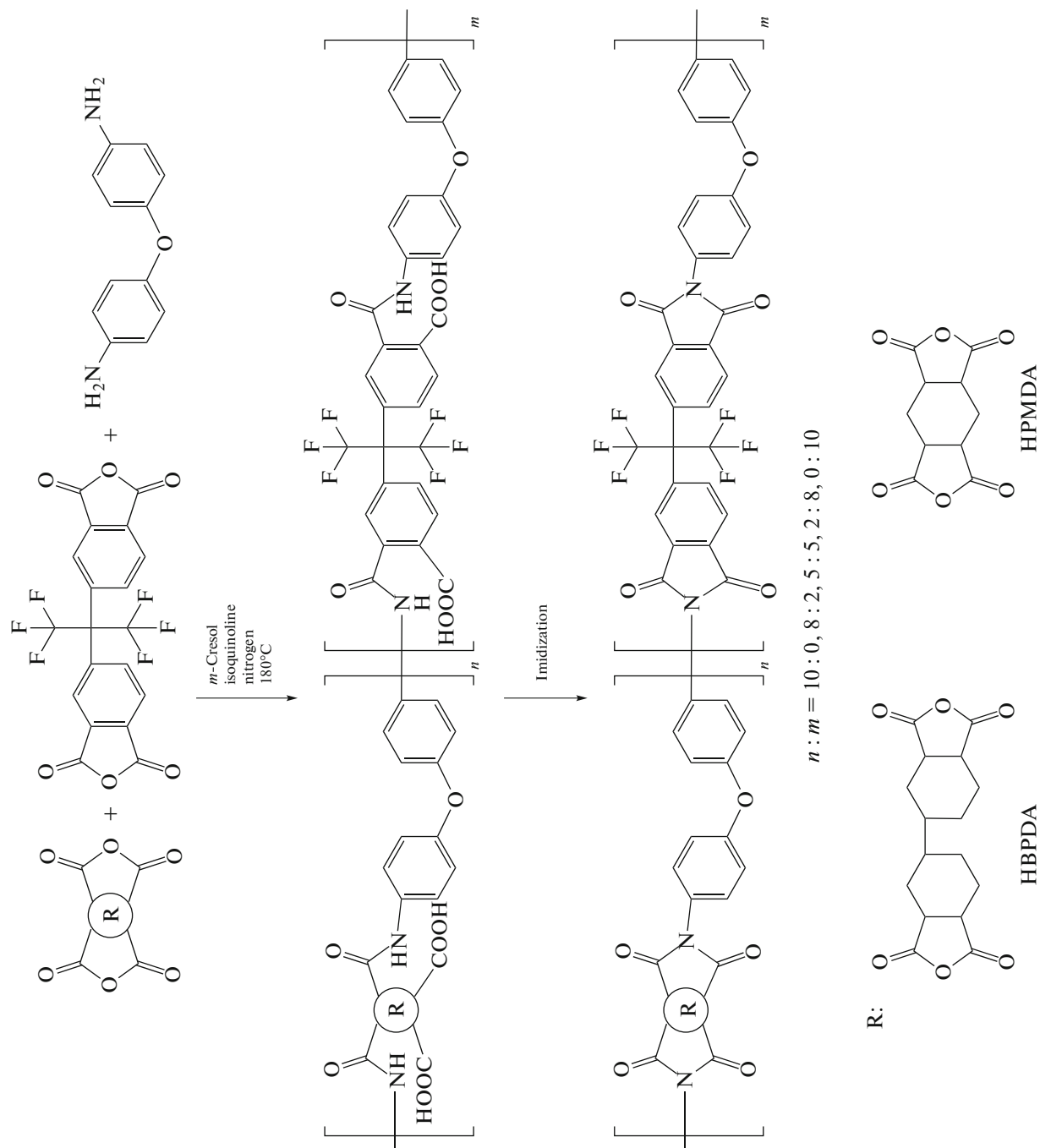
Characterization

The FTIR spectra of co-PI films were tested with a Tensor 27 (Bruker, Germany) apparatus with scanning times 32, and the scattering wavenumber in the range of 600 to 4000 cm⁻¹. A D8 Advance (Bruker, Germany) XRD device was used to analyze the degree of aggregation and dispersion of molecular chains within polymers. The mean spacing between molecular chains may be calculated employing Bragg's equation. Gel permeation chromatography (GPC) was performed with the instrument model Shimadzu LC-20AD (Shimadzu, Japan). DMAc was used as the mobile phase, and polystyrene was used as the standard. Shimadzu UV-3600 (Shimadzu, Japan) was used to test the light transmittance of the co-PI films in the wavelength range of 200 to 800 nm. The thermal stability of the films was tested using the STA449 (NETZSCH, Germany) TGA instrument at a heating rate of 10 K/min in nitrogen ranging from 50 to 800°C. The 204 F1 type DSC (NETZSCH, Germany) analyses was used to determine the glass transition temperature of the films in the temperature range 30 to 400°C, and the films were scanned twice at a heating rate of 10 K/min. The first time was utilized to remove the effect of thermal history, and the second test data was used as the final data. The coefficient of thermal expansion (CTE) of co-PI films was measured on a TMA Diamond SS6000 (Perkin Elmer, Germany) in the range of 50–200°C at a heating rate of 10 K/min in a dry nitrogen atmosphere. A 105D-7S type electronic universal testing machine (WANACE, China) was used at the tensile rate 5 mm/min, and the implementation standard was GBT1040.3-2006. Consequently, the average data from five sets of samples were utilized.

RESULTS AND DISCUSSION

Synthesis and Characterization of co-PI Films

As seen in Table 1, these co-PIs have high molecular weights and tend to increase as the 6FDA content increases due to the low reactivity of alicyclic dianhydride compared to 6FDA. These results show that CPI with moderate molecular weight have been successfully synthesized by copolycondensation [15]. In addi-



Scheme 1.

Table 1. Molecular weights and solubility of co-PI films

Sample	Molecular		Solubility				
	$M_n \times 10^{-4}$	\bar{D}	NMP	DMAc	THF	DCM	DMK
HBPDA-ODA	4.52	1.48	++	++	++	++	+ -
HBPDA/6FDA-82-ODA	4.81	1.59	++	++	++	++	+ -
HBPDA/6FDA-55-ODA	5.48	1.60	++	++	++	++	++
HBPDA/6FDA-28-ODA	5.87	1.62	++	++	++	++	++
6FDA-ODA	7.01	1.53	++	++	++	++	++
HPMDA/6FDA-28-ODA	5.74	1.67	++	++	++	++	++
HPMDA/6FDA-55-ODA	5.51	1.62	++	++	++	++	++
HPMDA/6FDA-82-ODA	5.14	1.47	++	++	++	++	+ -
HPMDA-ODA	4.71	1.41	++	++	++	++	+ -

(+ +) completely soluble, (+ -) partially soluble, (-) insoluble.

tion, the added 6FDA contains a larger bulky highly polar trimethyl group, which increases the spacing between inter/intramolecular chains, making the co-PI films soluble not only in high polarity solvents (NMP, DMAc), but also in low polarity solvents (THF, DCM) at room temperature. This is good for production and transportation [12].

A series of infrared characteristic absorption bands of the imide units can be observed in Fig. 1, including the asymmetric carbonyl stretching vibration of C=O at 1784 cm^{-1} and the symmetric carbonyl stretching vibration of C=O at 1710 cm^{-1} , and the C–N stretching vibration band at 1374 cm^{-1} . At the same time, there was no prominent absorption band of polyamic acid near 1660 and 1550 cm^{-1} , indicating that the imidization was complete. The stretching vibration

band of $-\text{CF}_3$ at 972 cm^{-1} is observed; with the increase of 6FDA content, the band intensity also increased, and the intensity of alicyclic on saturated C–H stretching vibration band at 2940 and 2860 cm^{-1} also decreased [26].

Molecular Simulation of HBPDA and HPMDA with 6FDA

In the current work, we simulated the conformation of the structural units of co-PI films using the MM2 Dynamics module of Chem3D software (version 19). Figure 2 shows the molecular simulation results. It was found that the addition of 6FDA increased the bond angle of the ether bond in the ODA molecule. The bond angle between the alicyclic struc-

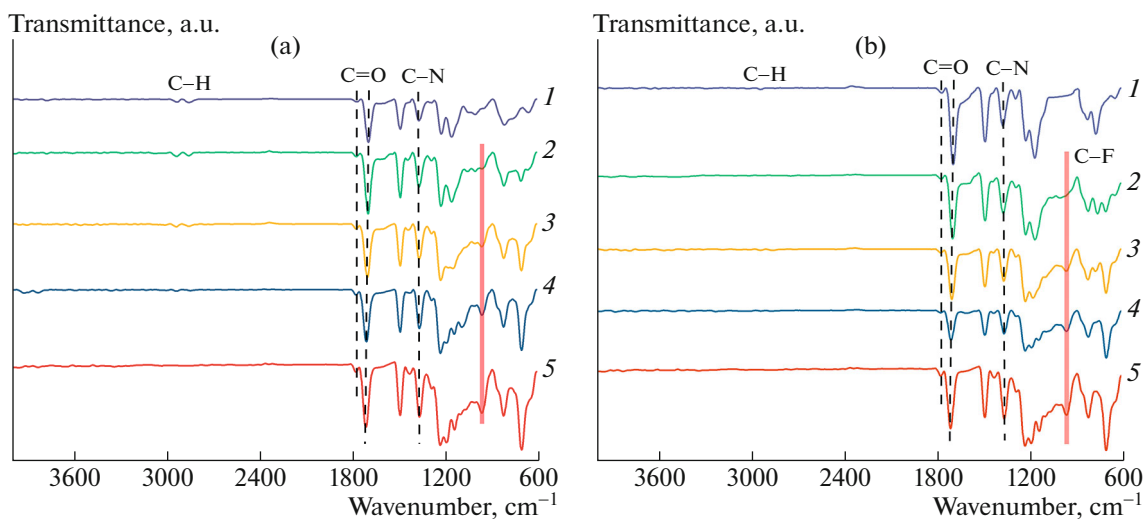


Fig. 1. ATR-FTIR spectra of (a) HBPDA-based co-PI: (1) HBPDA-ODA, (2) HBPDA/6FDA-82-ODA, (3) HBPDA/6FDA-55-ODA, (4) HBPDA/6FDA-28-ODA, (5) 6FDA-ODA and (b) HPMDA-based co-PI films: (1) HBMEDA-ODA, (2) HBMEDA/6FDA-82-ODA, (3) HBMEDA/6FDA-55-ODA, (4) HBMEDA/6FDA-28-ODA, (5) 6FDA-ODA.

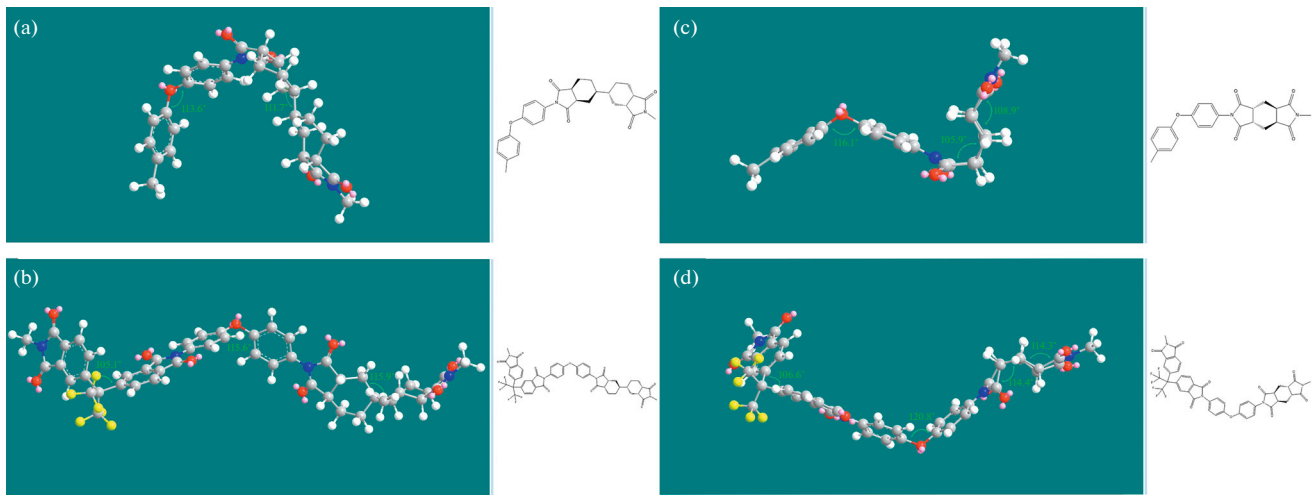


Fig. 2. Simulation of the structural unit conformation of co-PIs: (a) HBPDA-ODA, (b) HBPDA/6FDA-ODA, (c) HPMDA-ODA, (d) HPMDA/6FDA-ODA.

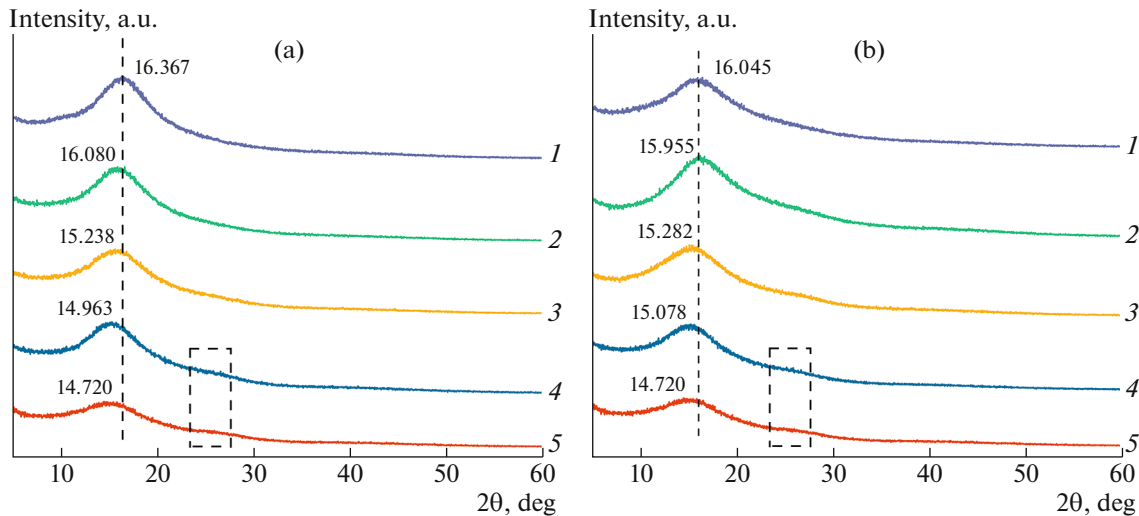


Fig. 3. XRD spectra of (a) HBPDA-co-PI films: (1) HBPDA-ODA, (2) HBPDA/6FDA-82-ODA, (3) HBPDA/6FDA-55-ODA, (4) HBPDA/6FDA-28-ODA, (5) 6FDA-ODA and (b) HPMDA-co-PI films: (1) HBMDA-ODA, (2) HBMDA/6FDA-82-ODA, (3) HBMDA/6FDA-55-ODA, (4) HBMDA/6FDA-28-ODA, (5) 6FDA-ODA.

ture reduced, which is conducive to improving the linearity of the molecular chains [13]. This is because 6FDA has a large trifluoromethyl group and ODA has flexible ether bonds, both of which reduce the symmetry and regularity of its polymer chains [30]. As a result, the spatial site resistance of the chains increases, which inhibits the stacking of molecular chains.

Aggregation Structure of co-PI films

The XRD spectra of two different co-PI films in Fig. 3 both shows a broad diffraction peak between

10° – 20° , indicating that PI exhibits an amorphous structure [31]. This is mainly due to the fact that the methyl group on 6FDA prevents the molecular chains from packing tightly together. Among all the above samples, 6FDA-ODA shown the longest average intermolecular chain distance of 6.013 \AA . With an increase in content of 6FDA, the average intermolecular chain distance of HBPDA and HPMDA series films increased by 0.504 and 0.352 \AA . Meanwhile, a weak peak appears near 25° , indicating an enhanced ordering of the molecular chains, which is consistent with the results of molecular simulation [27, 32].

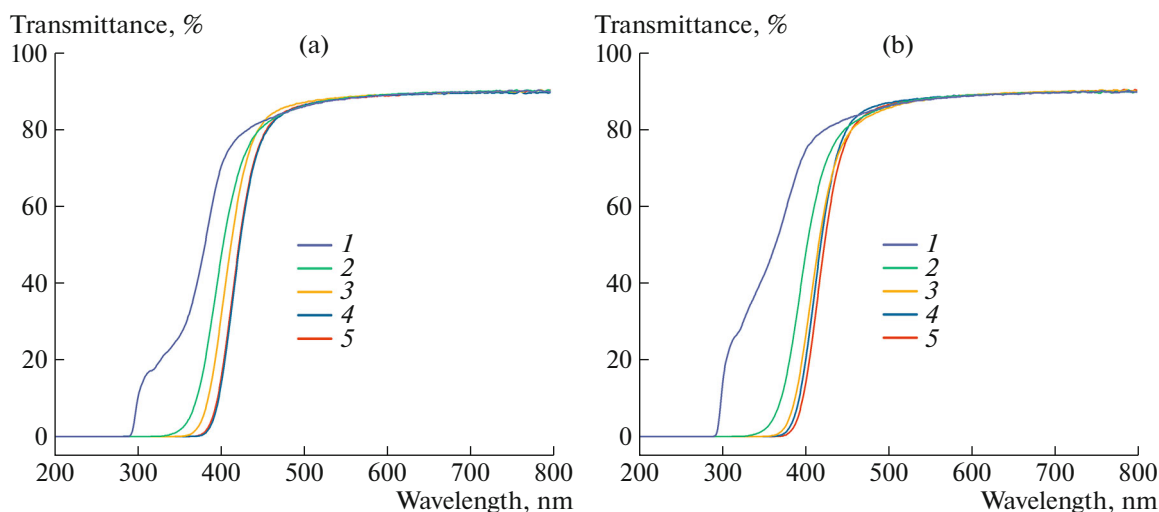


Fig. 4. UV–Vis spectra of (a) HBPDA-co-PI films: (1) HBPDA-ODA, (2) HBPDA/6FDA-82-ODA, (3) HBPDA/6FDA-55-ODA, (4) HBPDA/6FDA-28-ODA, (5) 6FDA-ODA and (b) HPMDA-co-PI films: (1) HBMDA-ODA, (2) HBMDA/6FDA-82-ODA, (3) HBMDA/6FDA-55-ODA, (4) HBMDA/6FDA-28-ODA, (5) 6FDA-ODA.

Optical Properties of co-PI Films

Figure 4 shows the ultraviolet-visible-near-infrared (UV–Vis) spectrum of the prepared co-PI films with the thickness of the tested films $\sim 35 \mu\text{m}$, and the key results are listed in Table 2. The cut-off wavelength of co-PI films is in the range of 288–362 nm. The transmittance at 450 nm is 77.3–82.7%, and the maximum transmittance reaches 90%. The cut-off wavelength of HPMDA series films is lower, which could be due to the lower content of methylene and methyne groups in HPMDA molecules than that in HBPDA [27]. This may also be due to the fact that the molecular chain spacing of HPMDA is larger than that of HBPDA, which is consistent with the XRD results. It can also be seen from Table 2 that the increase of 6FDA content did not show an obvious effect on the

transmittance of co-PI films in the high wavelength range, but the transmittance decreases in the low wavelength region. This is due to the $-\text{CF}_3$ group in 6FDA had a strong electron-withdrawing ability, which hinders the flow of electron clouds from the diamine to the dianhydride, so the formation of the charge transfer was effectively inhibited. But the aromatic backbone may still form some charge transfer, resulting in increased cutoff wavelength [12]. At the same time, the $-\text{CF}_3$ group has a larger volume, which increases the average spacing of the molecular chains in co-PIs and hinders the close packing of molecular chains, and makes the films maintain a high transmittance. The transmittance of the film prepared in this work is higher than that of the film prepared by Cosatchi [29].

Table 2. Optical properties of co-PI films

Sample	Transmittance, %			$\lambda_{\text{cut-off}}$, nm
	450 nm	500 nm	720 nm	
HBPDA-ODA	82.1	85.9	89.8	291
HBPDA/6FDA-82-ODA	80.5	86.1	89.9	315
HBPDA/6FDA-55-ODA	80.4	87.0	89.9	346
HBPDA/6FDA-28-ODA	78.3	86.3	89.5	361
6FDA-ODA	77.7	86.6	89.7	362
HPMDA/6FDA-28-ODA	80.2	86.8	89.7	356
HPMDA/6FDA-55-ODA	80.5	85.6	89.9	345
HPMDA/6FDA-82-ODA	80.7	86.1	89.7	310
HPMDA-ODA	82.7	86.0	89.6	288

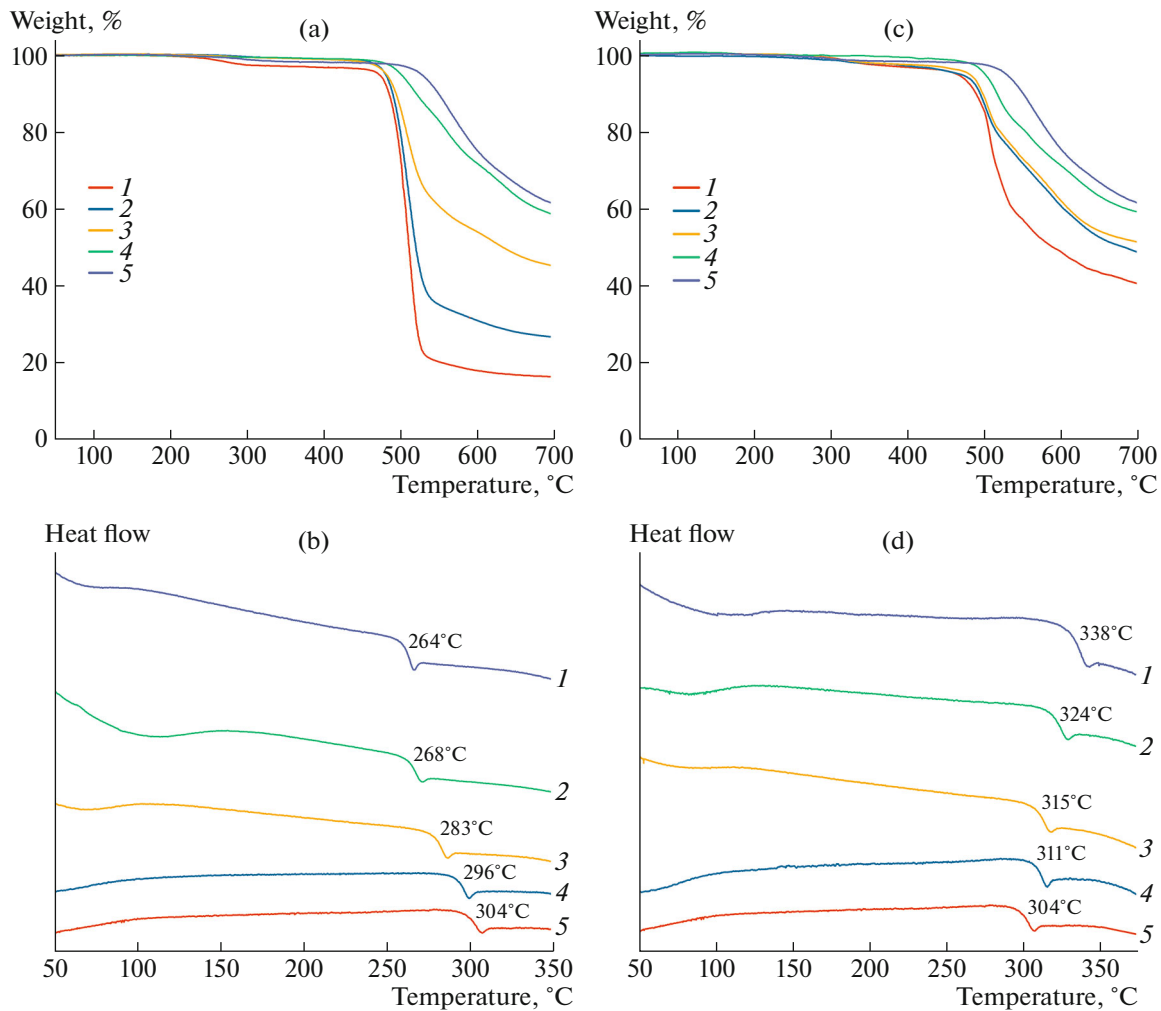


Fig. 5. (a, c) TGA and (b, d) DSC plots of (a, b) HBPDA-co-PI: (1) HBPDA-ODA, (2) HBPDA/6FDA-82-ODA, (3) HBPDA/6FDA-55-ODA, (4) HBPDA/6FDA-28-ODA, (5) 6FDA-ODA and (c, d) HPMDA-co-PI films: (1) HBMDA-ODA, (2) HBMDA/6FDA-82-ODA, (3) HBMDA/6FDA-55-ODA, (4) HBMDA/6FDA-28-ODA, (5) 6FDA-ODA.

Thermal Properties of co-PI Films

The TGA curves and corresponding thermal properties of co-PI films are shown in Fig. 5 and Table 3. The T_{HRI} and R_{700} of films from the HBPDA and HPMDA series increased by 38°C, 42.17%, and 34°C, 18.78%, suggesting that the addition of 6FDA effectively improved the thermal stability of the polyimide film. The bulky $-\text{CF}_3$ group in 6FDA restricts the movement of molecular chains, which may lead to increased thermal stability. However, the molecular rigidity of 6FDA is greater than HBPDA but less than HPMDA [15, 34]. Therefore, with the increase of 6FDA content, HBPDA series films of T_g continues to improve, HPMDA series films show opposite trend. Moreover, all co-PI films show good thermal stability with CTE values in the range of 48.1–54.7 ppm/K. This is mainly related to the intermolecular forces, rigidity, and linearity of main chains, which indicate

that the T_g and thermal stability of co-PI films are determined by a combination of factors [12]. The thermal stability of the film prepared in this work is higher than that of the film prepared by Lan and Li [14, 15].

Mechanical properties of co-PI films

The mechanical properties of co-PI films are shown in Table 4. All the co-PI films show high tensile strength in the range of 90–111 MPa, the tensile modulus is around 2.7–3.4 GPa, elongation at break is in the range of 4.7–8.7%. With the increase in 6FDA content, the tensile strength of the co-PI films increased and then decreased obviously. This is mainly due to the increase of 6FDA content makes the molecular weight and molecular chain rigidity of the films increase, as well as the greater chain entanglement and the orderliness of molecular chains are improved in the system. At the same time, the tensile strength of

Table 3. Thermal properties of co-PI films

Sample	T_g , °C	T_5 , °C	T_{30} , °C	R_{700} , %	T_{HRI} , °C	CTE, ppm/K
HBPDA-ODA	264	472	501	16.39	240	54.7
HBPDA/6FDA-82-ODA	268	480	506	26.74	243	53.9
HBPDA/6FDA-55-ODA	283	482	520	45.23	247	52.3
HBPDA/6FDA-28-ODA	296	501	612	58.56	278	50.6
6FDA-ODA	304	527	628	61.31	288	49.5
HPMDA/6FDA-28-ODA	311	500	606	59.05	277	52.2
HPMDA/6FDA-55-ODA	315	473	564	51.21	258	51.8
HPMDA/6FDA-82-ODA	324	467	557	48.52	255	49.7
HPMDA-ODA	338	463	516	40.27	243	48.1

Table 4. Mechanical properties of co-PI films

Sample	Tensile strength, MPa	Elasticity modulus, GPa	Elongation at break, %
HBPDA-ODA	90.3	2.69	8.69
HBPDA/6FDA-82-ODA	99.4	2.73	8.57
HBPDA/6FDA-55-ODA	109	3.11	6.93
HBPDA/6FDA-28-ODA	101	3.15	5.36
6FDA-ODA	92.6	2.98	4.72
HPMDA/6FDA-28-ODA	105	3.36	5.92
HPMDA/6FDA-55-ODA	111	3.41	6.58
HPMDA/6FDA-82-ODA	103	3.38	5.98
HPMDA-ODA	96.5	3.31	5.95

co-PI films decreases clearly as the interchain forces decrease with increasing average distance between molecular chains. Compared with the film prepared by Lan and Zuo, the co-PI films still show good mechanical performance [15, 35].

CONCLUSIONS

The poor mechanical properties and thermal stability of semi-alicyclic CPI film hinder their wider application. Although various methods have been reported to improve the comprehensive properties of CPI film, most of the results fall short of what is expected. In this work, commercial monomers can be used to prepare films with excellent properties by copolymerization, which was proved a feasible way by experimental results. In addition, the relationship between the structure and properties of polyimide was studied. We achieved a balance between transmittance, thermal stability, mechanical properties, and cost when the molar ratio of 6FDA and dianhydride is 1 : 1 and the comprehensive properties of the two series films are both optimal. With the addition of 6FDA, the T_{HRI} and R_{700} of HBPDA and HPMDA series films increased. The tensile strength increased in more than 15–20%. Although the cut-off wave-

length was increased, the transmittance of the film did not decrease noticeably (transparency up to 90%). Therefore, this study will have a good reference value for the preparation of transparent polyimide films with excellent comprehensive properties.

FUNDING

This work was supported by Innovative Research Group Project of the National Natural Science Foundation of China (no. 22035007).

CONFLICT OF INTEREST

The authors declare that they have no conflicts of interest.

REFERENCES

1. A. Susa, A. Mordvinkin, K. Saalwachter, S. van der Zwaag, and S. J. Garcia, *Macromolecules* **51**, 8333 (2018).
2. Q. Zhang, C.-Y. Tsai, L.-J. Li, and D.-J. Liaw, *Nature Commun.* **10**, 1239 (2019).
3. Y.-y. Tan, Y. Zhang, G.-l. Jiang, X.-x. Zhi, X. Xiao, L. Wu, Y.-j. Jia, J.-g. Liu, and X.-m. Zhang, *Polymers* **12**, 576 (2020).

4. Z.-h. Wang, G.-Q. Fang, J.-j. He, H.-x. Yang, and S.-y. Yang, *React. Funct. Polym.* **146**, 104411 (2020).
5. Y. Yang, J. H. Park, Y. Jung, S. G. Lee, S. K. Park, and S. Kwon, *J. Appl. Polym. Sci.* **134**, 44375 (2017).
6. C. Yi, W. Li, S. Shi, K. He, P. Ma, M. Chen, and C. Yang, *Solar Energy* **195**, 340 (2020).
7. X.-m. Zhang, Y.-z. Song, J.-g. Liu, and S.-y. Yang, *J. Photopolym. Sci. Technol.* **29**, 31 (2016).
8. S. A. A. Zaidi, J. Y. Song, J. H. Lee, S. M. Kim, and Y. Kim, *Mater. Res. Express* **6**, 086434 (2019).
9. P. Ma, C. Dai, H. Wang, Z. Li, H. Liu, W. Li, and C. Yang, *Compos. Commun.* **16**, 84 (2019).
10. M. Hasegawa, *Polymers* **9**, 520 (2017).
11. L. Qi, C.-Y. Guo, M.-G. Huang Fu, Y. Zhang, L.-m. Yin, L. Wu, J.-g. Liu, and X.-m. Zhang, *Polymers* **11**, 2055 (2019).
12. L. Tao, H. Yang, J. Liu, L. Fan, and S. Yang, *Polymer* **50**, 6009 (2009).
13. Z. Yang, H. Guo, C. Kang, and L. Gao, *Polym. Chem.* **12**, 5364 (2021).
14. P. Li, L. Liu, L. Ding, F. Lv, and Y. Zhang, *J. Appl. Polym. Sci.* **133**, 43081 (2016).
15. Z. Lan, C. Li, Y. Yu, and J. Wei, *Polymers* **11**, 1319 (2019).
16. B. V. Kotov, T. A. Gordina, V. S. Voishchev, O. V. Kolninnov, and A. N. Pravednikov, *Polym. Sci. U.S.S.R.* **19**, 711 (1977).
17. I. A. Novakov, B. S. Orlinson, D. V. Zav'yalov, S. V. Mednikov, E. N. Savel'ev, E. A. Potaenkova, M. A. Nakhod, A. M. Pichugin, A. V. Kireeva, and M. N. Kovaleva. *Rus. Chem. Bull.* **70**, 1141 (2021).
18. Y. Zhang, Y.-y. Tan, J.-g. Liu, X.-x. Zhi, M.-g. Huangfu, G.-l. Jiang, X. Wu, and X. Zhang, *J. Polym. Res.* **26**, 171 (2019).
19. Y. Yang, Y. Jung, M. D. Cho, S. G. Lee, and S. Kwon, *RSC Adv.* **5**, 57339 (2015).
20. P. K. Tapaswi and C.-S. Ha, *Macromol. Chem. Phys.* **220**, 1800313 (2019).
21. H. Gao, J. Li, F. Xie, Y. Liu, and J. Leng, *Polymer* **156**, 121 (2018).
22. M. A. Abdulhamid, X. Ma, B. S. Ghanem, and I. Pinnau, *ACS Appl. Polym. Mater.* **1**, 63 (2019).
23. A. Susa, J. Bijleveld, M. H. Santana, and S. J. Garcia, *ACS Sustain. Chem. Eng.* **6**, 668 (2018).
24. X. Hu, J. Yan, Y. Wang, H. Mu, Z. Wang, H. Cheng, F. Zhao, and Z. Wang, *Polym. Chem.* **8**, 6165 (2017).
25. J. Z. Huo and Y. F. Yu, *High Perform. Polym.* **31**, 394 (2019).
26. S. Wang, G. J. Yang, S. B. Wu, G. Ren, W. Yang, and X. K. Liu, *e-Polymers* **16**, 395 (2016).
27. X. Wu, G. L. Jiang, Y. Zhang, L. Wu, Y. J. Jia, Y. Y. Tan, J. G. Liu, and X. M. Zhang, *Polymers* **12**, 16 (2020).
28. A. Tundidor-Camba, C. Saldias, L. H. Tagle, C. A. Terraza, D. Coll, G. Perez, M. Aguilar-Vega, R. L. Abarca, and P. A. Ortiz, *J. Chil. Chem. Soc.* **63**, 4239 (2018).
29. A. I. Cosutchi, S.-L. Nica, C. Hulubei, M. Homocianu, and S. Ioan, *Polym. Eng. Sci.* **52**, 1429 (2012).
30. X.-X. Zhi, G.-L. Jiang, Y. Zhang, Y.-J. Jia, L. Wu, Y.-C. An, J.-G. Liu, and Y.-g. Liu, *J. Appl. Polym. Sci.* **139**, 51544 (2022).
31. G.-l. Jiang, D.-y. Wang, H.-p. Du, X. Wu, Y. Zhang, Y.-y. Tan, L. Wu, J.-g. Liu, and X.-m. Zhang, *Polymers* **12**, 413(2020).
32. T. L. Li and S. L. C. Hsu, *J. Phys. Chem. B* **114**, 6825 (2010).
33. R. Li, C. Ding, J. Yu, X. Wang, and P. Huang, *High Perform. Polym.* **33**, 905 (2021).
34. Z. Q. Hu, M. H. Wang, S. J. Li, X. Y. Liu, and J. H. Wu, *Polymer* **46**, 5278 (2005).
35. H. Zuo, Y. Chen, G. Qian, F. Yao, H. Li, J. Dong, X. Zhao, and Q. Zhang, *Eur. Polym. J.* **173**, 111317 (2022).